Charge-exchange processes in close atomic collisions

M. Meron* and B. Rosner
Department of Physics, Technion—Israel Institute of Technology, Haifa, Israel
(Received 11 October 1983)

Charge-exchange processes in small-impact-parameter collisions have been studied for systems consisting of C, N, O, Ne, and Ar ions, in the 0.5—1.8-MeV range. A "compound atom" model based on an assumption of a randomization of the electrons' motion during the collision was developed. It successfully reproduces the experimental distributions of the charge-states.

I. INTRODUCTION

Charge-exchange processes in atomic collisions are well-known phenomena since the early days of atomic physics. Over the years, the ever existing interest in charge distributions of ion beams passing through solid or gaseous targets spurred a large amount of research devoted to this subject.[1] As the equilibrium distributions are created mainly by multiple, large-impact-parameter collisions, it was this type of collision that received most of the attention. It is well known that the most probable charge-exchange processes in these "grazing" collisions are capture or loss of a single electron[1,2] through a direct Coulomb interaction. Those processes can be analyzed using an independent electron approximation[3] and ignoring the correlations between electrons except for the obvious screening effects.

The situation is much more complicated in small-impact-parameter collisions, where many electrons of both colliding atoms take part in the interaction, and a large charge change may occur even in a single collision. This was first observed in studies of close, low velocity ($v \ll 1$ a.u.) collisions, more than 20 years ago,[4,5] and explained, at least qualitatively, in the framework of the molecular orbitals model.[6–9] As is well known, the validity range of this model is limited by the condition $v \ll v_e$, when v_e is the equivalent orbital velocity of the electrons being considered. Therefore, at higher collision velocity ($v \gg 1$ a.u.) the molecular orbital (MO) model cannot be applied to the outer electrons of the colliding atoms. Of course, it may still be applicable for the inner electrons of both colliding atoms, unless v is exceedingly high, but their contribution to charge-exchange processes is minor in this case.[10,11]

Some experimental results concerning charge-exchange processes in close collisions, in the intermediate velocity range (1 a.u. $< v < Z$), were obtained over the last decade,[12,13] and they display rather peculiar features. It turns out that both loss and capture of a large number of electrons are quite probable in this case. Also the dependence of the post-collision charge distribution on the initial projectile's charge state and scattering angle is very weak.[12,13] The results indicate that the incoming and outgoing channels are almost decoupled, so that an equilibrium charge distribution is practically established in a single close collision. While being in a marked difference to the typical outcome of a single grazing collision, these results bear a strong resemblance to those of a multiple scattering in thick targets. This analogy was in fact the basis for one of the first models which were developed in order to explain those results.[14]

While the existing experimental data about charge exchange in close collisions are rather sparse, the theory is even more so, and for obvious reasons. The interactions in a typical close collision are so strong as to render a perturbative approach useless, while an independent electron approach seems to be ruled out by the experimental evidence for the decoupling of the incoming and outgoing interaction channels. A detailed theoretical treatment, based on first principles, of the multibody interactions in such a collision seems to be prohibitively difficult. On the other hand, just this complexity, and the experimental evidence mentioned above, seem to favor an approach based on statistical methods,[14] as it is done in the "compound nucleus" model,[15] in nuclear physics.

In an attempt to improve our understanding of charge-exchange processes in close atomic collisions, a study of these processes has been undertaken. In the first stage of this study, charge-state distributions resulting from close single collisions were measured for various colliding systems, as a function of the relevant physical parameters, i.e., collision velocity, impact parameter, and the initial projectile's charge state. The experimental results are displayed and discussed in Sec. II of this paper. Those results then served as a basis for the second stage which was devoted to the development of a model capable of a quantitative treatment of charge-exchange processes. The construction of this model is described in Sec. III, and a comparison between its predictions and the experimental results is shown in Sec. IV. In Sec. V a discussion of this model, and of its probable future development is presented.

II. EXPERIMENTAL RESULTS

Charge-state distributions of C, N, O, and Ne ions emerging from close single collisions with N_2, O_2, Ne, and Ar targets were measured as a function of the projectile energy E, initial charge state q_i, and scattering angle θ. The energy range was typically 0.5—1 MeV (equivalent to velocities in the 1.2—1.8 a.u. range) and in some cases up to 1.8 MeV. The range of q_i values was 0—3^+.

The scattering angles ranged from 0.3° to 5°, where the maximal angle for each data set was always chosen so as to make the corresponding impact parameter b value smaller than the K radii of the colliding atoms. The conversion of θ to b was accomplished assuming an exponentially screened Coulomb potential,[11] where the Thomas-Fermi scattering length,

$$a = 0.885(Z_1^{2/3} + Z_2^{2/3})^{-1/2} \text{ a.u.},$$

was used as the screening length.

Typical experimental errors were about 1% for $\langle q \rangle$, the average outgoing charge state, and 2—5 % for M_2, the second moment of the post-collision charge distribution relative to $\langle q \rangle$. The errors in the experimentally measured probabilities for various final charge states ranged from 1% for the dominant ones to ~10% for those with marginal probabilities. A detailed description of the experimental system and experimental procedures is being published elsewhere.[10,11]

One of the most noteworthy features of the experimentally measured charge-state distributions is their high degree of similarity for all target-projectile combinations. The distributions are always approximately symmetric (Fig. 1). The dependence of the results on q_i is rather weak, and usually systematic, namely increasing q_i by one unit results in a raise of the average final charge $\langle q \rangle$ in the order of 0.1 units (Figs. 2 and 3).

The dependence of the experimental results on the impact parameter b is rather weak (Figs. 2 and 3). Careful analysis showed that whatever b dependence exists, it can be attributed to the contribution of inner-shell excitations to the charge-exchange processes.[10,11] This contribution is

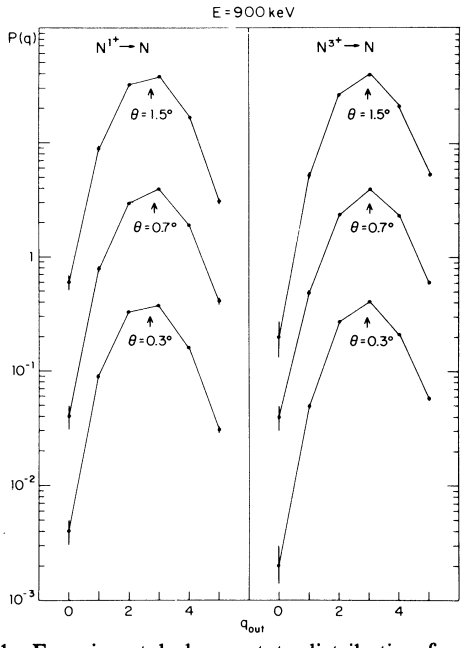

FIG. 1. Experimental charge-state distribution for N^{1+} and N^{3+} projectiles after a close single collision with the N_2 target for various scattering angles. The vertical scale relates to the lowest curve, while for each additional one the scale is moved up by one decade.

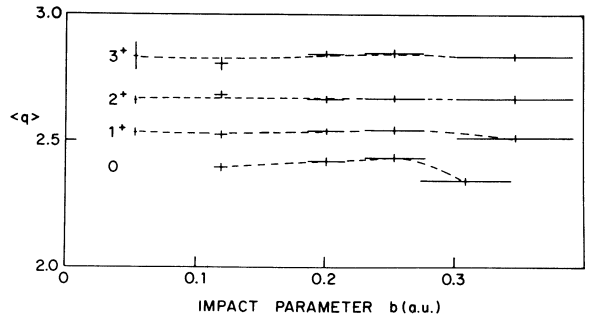

FIG. 2. $\langle q \rangle$ as a function of b for N projectiles colliding with Ar at 700 keV. The numbers adjacent to the curves are the projectiles q_i values.

superimposed on top of the much bigger (in our velocity range) and practically b-independent (for sufficiently small values of b) contribution of these processes in which the outer electrons of both atoms participate. As our main interest lies with the outer electron processes, a systematic procedure for the subtraction of the inner-shell contribution has been devised and applied to all our data. This procedure is described in separate publications.[10,11]

It should be mentioned, as it is of importance to the rest of this work, that the terms "inner" and "outer" electrons as used here have a dynamical meaning which depends on the collision velocity, and any given electron shell may be considered "inner" in one collision and "outer" in another. More about this subject in the next section.

A full listing of our results for $\langle q \rangle$ and M_2 as a function of projectile's atomic number Z_p, target's atomic number Z_T, collision velocity v, and q_i is displayed in Table I, after the subtraction of inner-shell excitations' contribution. The additional entries in this table are values calculated using the "compound-atom" model, which is discussed in the next section. We chose not to publish the full experimental charge-state distributions at this stage, so as not to complicate this work unnecessarily, but the data are available on request.

III. THE "COMPOUND-ATOM" MODEL

In view of our and other's[12] results for charge-exchange processes in close atomic collisions, it seems rather doubtful that an attempt of theoretical analysis based on an in-

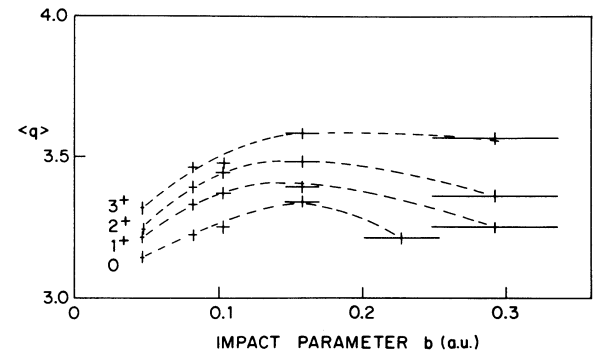

FIG. 3. Same as Fig. 2 for the symmetric colliding system Ne-Ne at 800 keV.

TABLE I. Comparison of $\langle q \rangle$ and M_2 values as obtained from the experimental distribution with values calculated using the compound-atom model. The contribution of inner-shell processes was subtracted from the experimental values wherever necessary.

Z_P	Z_T	v (a.u.)	q_i	$\langle q \rangle$ Experiment	$\langle q \rangle$ Model	M_2 Experiment	M_2 Model
6	7	1.41	0	2.30∓0.04	2.33	0.84∓0.04	0.74
6	7	1.41	1	2.35∓0.03	2.42	0.81∓0.04	0.73
6	10	1.41	0	2.51∓0.04	2.35	0.72∓0.05	0.79
6	10	1.41	1	2.63∓0.02	2.43	0.70∓0.04	0.78
6	10	1.41	2	2.76∓0.03	2.51	0.74∓0.04	0.77
6	10	1.63	1	2.63∓0.03	2.59	0.78∓0.03	0.84
6	10	1.83	0	2.50∓0.04	2.63	0.85∓0.05	0.89
6	10	1.83	1	2.59∓0.03	2.70	0.81∓0.04	0.88
6	10	1.83	2	2.73∓0.04	2.79	0.76∓0.03	0.87
6	10	1.83	3	2.85∓0.04	2.89	0.74∓0.04	0.85
7	7	1.20	0	2.41∓0.03	2.29	0.85∓0.05	0.71
7	7	1.20	1	2.47∓0.03	2.38	0.83∓0.03	0.71
7	7	1.20	2	2.52∓0.03	2.49	0.86∓0.03	0.69
7	7	1.20	3	2.57∓0.03	2.63	0.89∓0.05	0.67
7	7	1.41	0	2.48∓0.03	2.53	0.90∓0.05	0.78
7	7	1.41	1	2.56∓0.03	2.63	0.87∓0.03	0.78
7	7	1.41	2	2.66∓0.03	2.73	0.91∓0.04	0.76
7	7	1.41	3	2.77∓0.03	2.86	0.93∓0.05	0.75
7	7	1.60	0	2.61∓0.04	2.70	0.95∓0.05	0.83
7	7	1.60	1	2.66∓0.02	2.80	0.94∓0.03	0.82
7	7	1.60	2	2.77∓0.03	2.90	0.94∓0.04	0.81
7	7	1.60	3	2.91∓0.03	3.02	0.95∓0.05	0.80
7	8	1.41	0	2.58∓0.03	2.57	1.00∓0.05	0.80
7	8	1.41	1	2.68∓0.02	2.66	1.03∓0.02	0.80
7	10	1.41	1	2.88∓0.04	2.68	0.80∓0.03	0.83
7	10	1.60	1	3.00∓0.03	2.86	0.90∓0.02	0.89
7	18	1.20	0	2.32∓0.03	2.28	0.75∓0.04	0.83
7	18	1.20	1	2.44∓0.03	2.36	0.70∓0.03	0.83
7	18	1.20	2	2.55∓0.03	2.45	0.68∓0.04	0.81
7	18	1.20	3	2.73∓0.04	2.57	0.71∓0.05	0.80
7	18	1.41	0	2.41∓0.04	2.51	0.72∓0.05	0.92
7	18	1.41	1	2.54∓0.02	2.59	0.74∓0.04	0.92
7	18	1.41	2	2.66∓0.03	2.68	0.73∓0.04	0.91
7	18	1.41	3	2.82∓0.03	2.79	0.72∓0.04	0.89
7	18	1.60	0	2.63∓0.03	2.68	0.80∓0.04	0.99
7	18	1.60	1	2.72∓0.03	2.76	0.82∓0.02	0.98
7	18	1.60	2	2.81∓0.03	2.85	0.82∓0.03	0.97
7	18	1.60	3	2.94∓0.04	2.95	0.82∓0.04	0.96
8	7	1.41	1	2.70∓0.04	2.68	0.82∓0.03	0.82
8	7	1.41	1	2.79∓0.03	2.79	0.80∓0.02	0.81
8	8	1.41	0	2.73∓0.03	2.74	0.94∓0.04	0.84
8	8	1.41	1	2.89∓0.03	2.84	0.92∓0.02	0.84

TABLE I. (*Continued*).

Z_P	Z_T	v (a.u.)	q_i	$\langle q \rangle$ Experiment	$\langle q \rangle$ Model	M_2 Experiment	M_2 Model
8	18	1.41	0	2.75∓0.03	2.77	0.81∓0.04	0.97
8	18	1.41	1	2.85∓0.03	2.84	0.79∓0.02	0.97
10	7	1.41	0	3.21∓0.03	2.89	0.80∓0.03	0.87
10	7	1.41	1	3.35∓0.03	3.00	0.83∓0.03	0.87
10	7	1.90	2	3.88∓0.03	3.69	0.89∓0.03	1.01
10	10	1.18	1	2.92∓0.03	2.84	0.95∓0.04	0.83
10	10	1.26	0	2.87∓0.06	2.89	0.97∓0.05	0.88
10	10	1.26	1	2.90∓0.04	2.98	0.98∓0.04	0.88
10	10	1.26	2	2.97∓0.05	3.08	1.01∓0.04	0.87
10	10	1.26	3	3.10∓0.06	3.20	1.06∓0.06	0.85
10	10	1.41	0	3.05∓0.05	3.12	0.92∓0.04	0.95
10	10	1.41	1	3.12∓0.04	3.21	0.93∓0.03	0.94
10	10	1.41	2	3.15∓0.05	3.31	0.97∓0.03	0.93
10	10	1.41	3	3.26∓0.05	3.43	1.02∓0.04	0.92
10	10	1.90	2	3.93∓0.03	3.92	1.08∓0.02	1.11

dependent electron approximation may be successful. On the other hand, those results bear a strong reminiscence of the compound-nucleus processes in nuclear physics,[15] at least as far as the decoupling of incoming and outgoing interaction channels is considered. While both cases are not similar, this resemblance may serve as a guideline for the development of a model capable of a quantitative treatment of charge-exchange processes in close collisions. Such a model was in fact developed and is presented here.

The main assumption of this model is that during a close collision those outer electrons of both atoms which are not altogether thrown out of the system create a common structureless electron cloud which is later redistributed between both atoms. The inner electrons, at the same time, remain relatively inert and follow "their" atoms, with the possible exception of promotion processes through couplings between molecular orbitals. This chain of events is shown in Fig. 4.

In order to turn this assumption into a quantitative model, a few questions should be answered.

(1) Under what circumstances can such an electron cloud be created?

(2) What is the border line between inner and outer electrons in a given collision?

(3) How many electrons remain in the common cloud to be redistributed?

(4) According to what rules is the redistribution accomplished?

We shall answer those questions one by one. First, it should be understood that the creation of the common electron cloud means a randomization of the motion of the outer electrons. Such a randomization cannot take place when v, the collision velocity, is too small ($v<1$ a.u.) as in this case all the electrons occupy fairly well-defined orbitals during the collision and the process is nearly adiabatic. On the other hand, when v is much greater than the average electronic velocity in the colliding atoms, the electron-electron cross sections become too small to allow for a significant randomization to take place. By "electronic velocity" we naturally mean the equivalent velocity u defined by the binding energy E_B through

$$\frac{u^2}{2} = |E_B| \ , \tag{1}$$

and its average, as given by the Thomas-Fermi model, or in fact any semiclassical model of atomic structure, is of the order of $Z^{2/3}$, where Z is the atomic number. Therefore a reasonable, though crude, estimate of the validity range of the randomization assumption is given by

$$1 < v < Z_m^{2/3} \ , \tag{2}$$

where $Z_m = \min(Z_P, Z_T)$.

To answer the second question, we wish to define some cutoff electronic velocity $u_c(v)$, so that the outer electrons are those with $u < u_c$. One has to bear in mind, however, that the transition between inner and outer electrons is really a gradual one, and the use of a sharp boundary between them is just a rough approximation reflecting our lack of information about the real state of matters during the collision. Therefore it is unreasonable to assume that a sharp estimate for u_c can be obtained from a first-principles calculation. More realistic options are either to leave u_c as a free parameter in the model, or to try to obtain a reasonable estimate for it on the basis of qualitative arguments and general trends in the experimental data. The second of these options was realized here by invoking

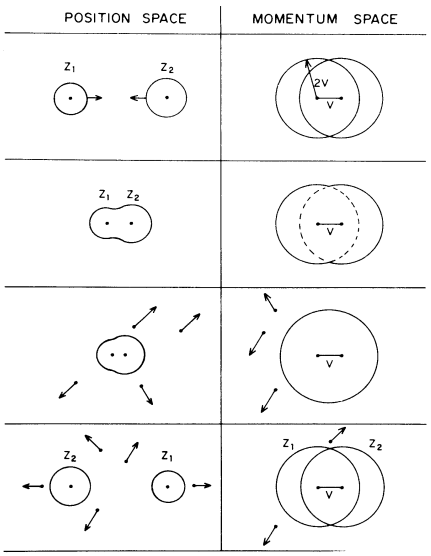

FIG. 4. Schematic view of close atomic collision in position and momentum space, according to the compound-atom model.

the uncertainty principle for the simplified case of the Bohr atom. During a collision at velocity v the energy of an electron at energy level n is defined up to

$$\Delta E_n \approx \frac{1}{\Delta t} \approx \frac{v}{r_n} \tag{3}$$

where r_n is the radius of the electron's orbit. When the sum of the uncertainties for two adjacent levels is of the order of the energy difference between them, it can be said that those electrons do not occupy well-defined orbitals during the collision, and therefore, according to our nomenclature are considered outer. Therefore the "borderline" between inner and outer electrons is defined approximately by

$$\frac{2v}{r_n} \approx \Delta E_n + \Delta E_{n+1} \approx -\frac{d}{dn}\left[\frac{Z^2}{2n^2}\right] = \frac{Z^2}{n^3} = \frac{u_n}{r_n} , \tag{4}$$

where the relations $u_n = Z/n$ and $r_n = n^2/Z$ were used. As the value of the electron velocity u_n in this case is just the u_c we are looking for, it follows immediately that

$$u_c \simeq 2v . \tag{5}$$

Crude as it is, this estimate seems to be in quite a good agreement with the experimental data, and therefore it is used throughout this work.

To make use of this result we define the function $Z(u)$, which is the number of electrons in an atom with atomic number Z whose velocities are smaller than u (or, equivalently, the effective charge of a nucleus when screened by the electrons with velocities greater than u). Obviously, the initial number of electrons in the common cloud N_i is given by

$$N_i = Z_1(u_c) + Z_2(u_c) - q_i . \tag{6}$$

$Z(u)$ is obtained as follows: In the Bohr atom model the screened nuclear charge, felt by an electron at level n, is given by

$$Z(n) \approx Z - \frac{2n^3}{3} , \tag{7}$$

where the factor $2n^3/3$ is approximately the number of electrons with principal quantum number smaller than n plus half the number of electrons at level n. This model yields also the relation $nu = Z$ which can be generalized to

$$nu = Z(n) . \tag{8}$$

Combining Eqs. (4) and (5) and substituting $Z(u)$ for $Z(n)$ we obtain

$$Z^3(u) + \tfrac{3}{2}u^3[Z(u) - Z] = 0 . \tag{9}$$

A good approximation for the exact solution of Eq. (9) is given by

$$Z(u) \approx \frac{Zu}{[u^2 + (\frac{2}{3}Z^2)^{2/3}]^{1/2}} . \tag{10}$$

It is worth mentioning that the function $F(u) = (d/du)Z(u)$, which is the electrons velocity distribution function, is roughly constant for $u < Z^{2/3}$.

N_f, the number of electrons remaining in the cloud, which is the essence of the third question, can be derived by the following integral:

$$N_f = \int_{u_m}^{u_c} F_c(u)[1 - P_I(u)]du , \tag{11}$$

where $F_c(u)$ is the velocity distribution of the electrons in the cloud, u_m and u_c are the lower and upper velocity limits for this distribution, and $P_I(u)$ is the ionization probability of an electron in the cloud.

A reasonable first estimate for the lower velocity limit is a weighted average of v_1 and v_2, the velocities of the Z_1 and Z_2 ions relative to the center-of-mass system in which the cloud is stationary

$$u_m(0) = \frac{Z_1(u_c)v_1 + Z_2(u_c)v_2}{Z_1(u_c) + Z_2(u_c)} . \tag{12}$$

However, it should be taken into account that u_m is expected to be an increasing function of q_i, which approaches u_c in the limit of $q_i = Z_1(u_c) + Z_2(u_c)$. ($N_i$ tends to zero in the same limit.) The simplest improved estimate for u_m which takes those facts into account is the following linear combination of $u_m(0)$ and u_c:

$$u_m = \frac{N_i u_m(0) + q_i u_c}{N_i + q_i} . \tag{13}$$

Now, according to the previous remark, $F_c(u)$, the velocity distribution of the outer electrons in a compound atom with $Z = Z_1 + Z_2$, is approximately constant for the range of u given by Eqs. (2) and (5). Therefore, normalizing $F_c(u)$ to N_i and substituting in Eq. (11) we obtain

$$N_f = \frac{N_i}{u_c - u_m} \int_{u_m}^{u_c} [1 - P_I(u)]du . \tag{14}$$

The ionization probability $P_I(u)$ is computed using a semiclassical approximation. First, we calculate the clas-

sical momentum transfer to an electron moving in a circular orbit with radius r and velocity u due to the Coulomb interaction with charge Z that moves with velocity v and passes through the center of the electron's orbit. The calculation, details of which are described in Appendix A, yields

$$|\Delta\bar{P}| = \frac{2Z}{rv}\left[\frac{u}{v}K_1\left(\frac{u}{v}\right)\right], \tag{15}$$

where $K_1(x)$ is a modified Bessel function. Now, an electron in the cloud interacts with two ions, possessing effective charges $Z_1(u_c)$ and $Z_2(u_c)$ and moving with velocities v_1 and v_2, respectively. Utilizing the virial relation for such an electron,

$$Z_1(u_c)+Z_2(u_c)\approx ru^2 ,$$

we obtain the total momentum transfer

$$|\Delta\bar{P}| = \frac{2u}{Z_1(u_c)+Z_2(u_c)}\left[Z_1(u_c)\left(\frac{u}{v_1}\right)^2 K_1\left(\frac{u}{v_1}\right) + Z_2(u_c)\left(\frac{u}{v_2}\right)^2 K_1\left(\frac{u}{v_2}\right)\right]. \tag{16}$$

This $|\Delta\bar{P}|$ and the well-known fact that the average energy transfer in a semiclassical approximation equals the classical energy transfer, yields

$$\frac{u^2}{2}P_I^0(u)\approx\frac{|\Delta\bar{P}|^2}{2},\quad P_I^0(u)\approx\left(\frac{\Delta\bar{P}}{u}\right)^2 \tag{17}$$

where transitions to bound states are ignored, and it is assumed that ionization processes do not take energy in excess of the ionization energy.

This result for $P_I(u)$ is at best a first-order approximation. It does not take into account the cutoff that has been introduced at $u=u_c$, and due to the approximations made during its calculation there is nothing to stop it from becoming bigger than one (albeit under rather rare circumstances). The first problem can be taken care of by multiplying $P_I^0(u)$ by a factor of $1-(u/u_c)^2$. As for the second problem, it has to be remembered that even if we are dealing with a single atomic collision, from the point of view of the electron it is a multiple collision process, much like a passage through a solid target. Therefore if the process is divided into n steps, and it is assumed that $P_I^0(u)/n$ is the ionization probability per step, the estimate for $P_I(u)$ is improved as follows:

$$P_I(u)\approx 1-\left[1-\frac{P_I^0(u)}{n}\right]^n \to 1-e^{-P_I^0(u)} \quad \text{as } n\to\infty . \tag{18}$$

While it hardly matters as long as $P_I^0(u)$ is reasonably small, this new form keeps $P_I(u)$ from becoming greater than unity. Now combining (18) with (17) and introducing the cutoff factor we arrive at the final expression,

$$P_I(u)=1-\exp\left\{-\left(\frac{\Delta P}{u}\right)^2\left[1-\left(\frac{u}{u_c}\right)^2\right]\right\}. \tag{19}$$

By substituting $P_I(u)$ from (19) into (14) and using (5), (6), and (13), N_f can be readily computed.

The fourth and last question deals with the redistribution of those N_f electrons between the colliding atoms. Here the simplest and most natural assumption is that the redistribution process is binomial, with a fixed probability for any electron to get caught into either one of the ions. However, it turns out that no choice of parameters for a binomial distribution enables it to reproduce in the same time the first and second moments of the experimental charge distributions, and in addition to account for the fact that the experimental distributions are very nearly symmetric. Therefore, as the next simplest possibility we assume that the capture processes are consecutive, and the probability for each electron to be caught into any of the ions is proportional to the (screened) charge of this ion. In other words, the capture probabilities of an electron into ions Z_1 and Z_2 which already caught k_1 and k_2 electrons are given by

$$\Pi_{1,2}=\frac{Z_{1,2}-k_{1,2}}{Z_1+Z_2-(k_1+k_2)} . \tag{20}$$

Those probabilities can be used to find P_k^n, the probability that out of n electrons k_1 are caught into Z_1 and $(n-k_1)$ into Z_2. Details of the calculation can be found in Appendix B. The result is

$$P_{k_1}^n=\frac{\begin{bmatrix} n \\ k_1 \end{bmatrix}\begin{bmatrix} Z_1+Z_2-n \\ Z_1-k_1 \end{bmatrix}}{\begin{bmatrix} Z_1+Z_2 \\ Z_1 \end{bmatrix}} . \tag{21}$$

In using the probabilities $P_{k_1}^n$ to obtain the final charge distribution, $Z_1(u_c)$ and $Z_2(u_c)$ should be substituted for Z_1 and Z_2. As their values are not integral, γ functions should be used instead of factorials in Eq. (21). Furthermore, we must take into account that, according to the Bohr principle, the motion of the ions relative to the electron cloud prevents electron capture into orbitals with velocities smaller than the ion velocity. Using again the approximation of constant states' density, this can be introduced into the model by multiplying the probabilities $\Pi_{1,2}$ by $(1-v_1/u_c)$ and $(1-v_2/u_c)$, respectively, and adding a probability for an electron not to be caught in any of the ions. By a proper redefinition of Z_1 and Z_2, the new probabilities can be brought back into form identical to $\Pi_{1,2}$, so that the problem remains solvable. As the distributions are very similar to Gaussian, they can be characterized to a good approximation by their first and second moments alone. To save space only those results are given here.

The result for N_1, the average number of electrons caught into Z_1, is

$$N_1=\frac{N+Z_1(u_c)}{Z_1(u_c)+Z_2(u_c)}\left[1-\frac{v_1}{u_c}\right] . \tag{22}$$

Subtracting N_1 from $Z_1(u_c)$, the charge state of this ion before the capture process, yields the final average charge state

$$\langle q \rangle_1 = Z_1(u_c) - N_1 \ . \tag{23}$$

The second moment of the distribution relative to $\langle q \rangle$ is

$$(M_2)_1 = \frac{N_1 \left[1 - \frac{N_1}{N_f}\right] \left[1 - \frac{N_1}{Z_1(u_c)}\right]}{1 - \frac{N_1}{N_f Z_1(u_c)}} \ . \tag{24}$$

IV. COMPARISON OF THE EXPERIMENTAL RESULTS TO THE PREDICTIONS OF THE COMPOUND-ATOM MODEL

The additional entries in Table I, besides the experimental results, are values of $\langle q \rangle$ and M_2 as calculated using the compound-atom model. This allows a direct comparison between experimental and calculated results. It can be seen that the agreement is quite good for the projectile-target systems and energy range presented in this study.

A more visual, if fragmentary, picture can be obtained from Figs. 5–7. In Fig. 5 full charge-state distributions of N ions for two different values of q_i, and two different targets are compared with their theoretical counterparts, and the agreement is very good. In Figs. 6 and 7 the compound-atom model's predictions for $\langle q \rangle$ and M_2 are compared with the experimental values for fixed Z_p in the first case, and for fixed Z_T in the second. Here too the agreement seems to be quite good, even if additional data points could give a better picture. Unluckily, the fact that the Technion Van de Graaf accelerator can accelerate only substances available as gases at ambient temperature, and the same is true about the targets, severely limited the number of target-projectile combinations that could be studied. Therefore, additional experiments of this kind have to be performed on other accelerators, in order to provide a broader data set for comparison with the theoretical results.

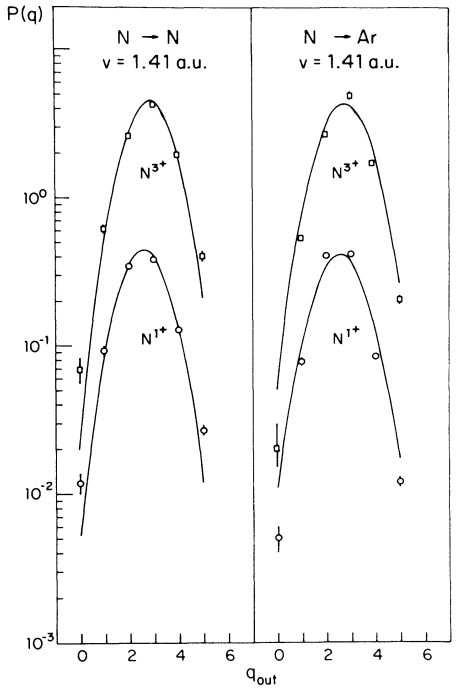

FIG. 5. Charge-state distributions resulting from close collisions of N ions with N_2 and Ar targets at $v=1.41$ a.u. The circles and squares represent experimental results for $q_i=1$ and $q_i=3$, respectively. The solid curves are obtained using the compound-atom model. The vertical scale is shifted by one decade for the $q_i=3$ case.

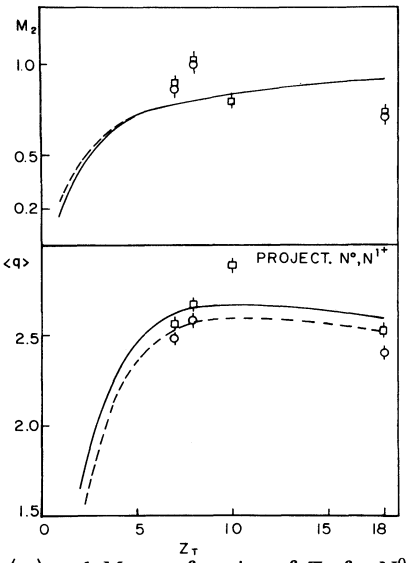

FIG. 6. $\langle q \rangle$ and M_2 as a function of Z_T for N^0 (circles) and N^{1+} (squares) projectiles. The lines are obtained using the compound-atom model, where the solid line corresponds to N^{1+}

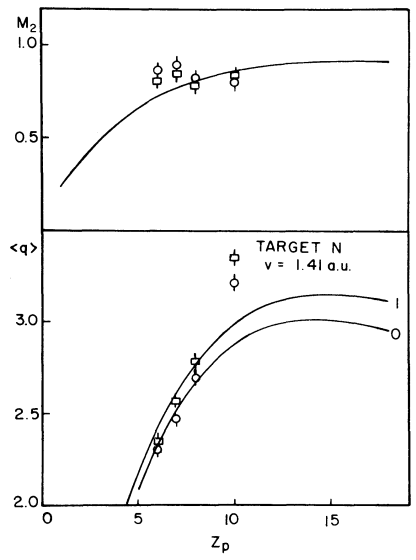

FIG. 7. $\langle q \rangle$ and M_2 as a function of Z_P for N_2 target. The q_i values are 0 (circles) and 1^+ (squares). The lines are obtained from the model.

In fact a recent study in which similar experiments with N projectiles over the 1.5—3.0-MeV energy range on N_2, Ne, Ar, Kr, and Xe targets was reported.[16] At the lower energy the experimental results agree with the model even for the heaviest targets. At the highest energy ($v \sim 3$ a.u.) small deviation starts to occur. The experimental $\langle q \rangle$ becomes larger than the predicted value and the M_2 narrower.

V. DISCUSSION AND CONCLUSIONS

The compound-atom model succeeds quite well in reproducing our experimental data. While statistical models for close atomic collisions were already developed in the past,[17,18] this is to the best of our knowledge the first one which succeeds in reproducing the shapes of the charge distributions without using any adjustable parameters. Of course, it would be premature to claim that the model is perfect in its present form. However, before any decisions about future directions of attack are made, more experimental data about close atomic collisions is needed. Especially, as the model determines the final charge distributions for both projectile and target atoms, data from experiments in which both distributions are measured would be helpful.

When discussing the present form of the model and possible future refinements, a clear distinction has to be made between its essential and secondary features. The essential part consists of the basic assumptions that during the collision the outer electrons of both atoms are first mixed together and then redistributed among bound states in both atoms and unbound states in the continuum. It is our opinion that those assumptions are necessary in order to explain the experimentally observed features of charge distributions resulting from close atomic collisions. All the other assumptions and approximations which are used for calculations in the framework of the model have to be viewed as secondary "tools" which may be refined and/or simplified when, and if, possible. Especially it is conceivable that the sharp cutoff at $u_c = 2v$ will have to be relaxed, and exchanged for a more realistic cutoff which will take into account the differences between the colliding atoms for the case of asymmetric collisions. Also the estimates for ionization probabilities, and for the number of electrons thrown out during the collision, can possibly be improved. While any such refinement, if possible, will improve the model by allowing it to achieve a still better agreement with a larger class of experimental phenomena, it will not change the basic structure of the model and its physical content.

ACKNOWLEDGMENTS

The authors wish to thank Dr. I. Gertner, Dr. D. Maor, and Dr. A. Mann for many helpful discussions and Mr. I. Saban for the smooth operation of the accelerator.

APPENDIX A: CLASSICAL MOMENTUM TRANSFER TO AN ELECTRON IN A CIRCULAR ORBIT

The situation we are dealing with here is of an electron moving in a circular orbit, with radius r and angular velocity ω in the x-y plane, while an ion with charge z is moving along a straight line passing through the center of the electron orbit, with a velocity v.

The positions of the electron and the ion in time t are, respectively,

$$\bar{r}(t) = r[\hat{x}\cos(\omega t) + \hat{y}\sin(\omega t)] , \tag{A1}$$

and

$$\bar{R}(t) = vt\hat{z} . \tag{A2}$$

The momentum transfer to the electron is simply

$$\Delta\bar{P} = Z\int_{-\infty}^{\infty} \frac{[\bar{R}(t)-\bar{r}(t)]}{[\bar{R}(t)-\bar{r}(t)]^3} dt . \tag{A3}$$

Substitution of (A1) and (A2) into (A3) yields

$$\Delta\bar{P} = Z\int_{-\infty}^{\infty} \frac{vt\hat{z} - r[\hat{x}\cos(\omega t) + \hat{y}\sin(\omega t)]}{(r^2+v^2t^2)^{3/2}} dt . \tag{A4}$$

As the denominator is an even function of t, the contribution of the odd terms in it vanishes. Therefore

$$\Delta\bar{P} = -rZ\hat{x}\int_{-\infty}^{\infty} \frac{\cos(\omega t)}{(r^2+v^2t^2)^{3/2}} dt . \tag{A5}$$

Now the substitution $t = (r/v)y$ yields

$$\Delta\bar{P} = \frac{2Z\hat{x}}{rv}\int_0^{\infty} \frac{\cos(\lambda y)}{(1+y^2)^{3/2}} dy , \tag{A6}$$

where $\lambda = \omega r/v = u/v$ and u is the orbital velocity of the electron. The integral in (A6) is known and its value is $\lambda K_1(\lambda)$,[19] where K_1 is a modified Bessel function of the third kind and first order. Substitution of this value into (A6) yields the final result for the absolute value of the momentum transfer:

$$|\Delta\bar{P}| = \frac{2Z}{rv}\left[\frac{u}{v}K_1\left[\frac{u}{v}\right]\right] . \tag{A7}$$

APPENDIX B: IMPORTANT RELATIONS FOR THE HYPERGEOMETRIC DISTRIBUTION

In Sec. III, Eq. (20), the capture probabilities of an electron into ions Z_1 and Z_2 which already caught k_1 and k_2 electrons, respectively, are given as

$$\Pi_1 = \frac{Z_1-k_1}{Z_1+Z_2-(k_1+k_2)} ,$$
$$\Pi_2 = \frac{Z_2-k_2}{Z_1+Z_2-(k_1+k_2)} . \tag{B1}$$

Therefore, $P^n_{k_1}$, the probability that k_1 out of n electrons are caught into Z_1 and the remaining $n-k_1$ into Z_2, has to satisfy the following difference equation:

$$P^n_{k_1} = P^{n-1}_{k_1-1}\frac{Z_1-k_1+1}{(Z_1+Z_2-n+1)} + P^{n-1}_{k_1}\frac{Z_2-n+k_1+1}{(Z_1+Z_2-n+1)} . \tag{B2}$$

We assume a solution of the form

$$P_{k_1}^n = \frac{\begin{bmatrix} n \\ k_1 \end{bmatrix} \begin{bmatrix} Z_1+Z_2-n \\ Z_1-k_1 \end{bmatrix}}{\begin{bmatrix} Z_1+Z_2 \\ Z_1 \end{bmatrix}} . \tag{B3}$$

Substitution of (B3) into (B2) yields

$$\begin{bmatrix} n \\ k_1 \end{bmatrix} \begin{bmatrix} Z_1+Z_2-n \\ Z_1-k_1 \end{bmatrix} = \begin{bmatrix} n-1 \\ k_1-1 \end{bmatrix} \begin{bmatrix} Z_1+Z_2-n+1 \\ Z_1-k_1+1 \end{bmatrix} \frac{Z_1-k_1+1}{Z_1+Z_2-n+1} + \begin{bmatrix} n-1 \\ k_1 \end{bmatrix} \begin{bmatrix} Z_1+Z_2-n+1 \\ Z_1-k_1 \end{bmatrix} \frac{Z_2-n+k_1+1}{Z_1+Z_2-n+1} . \tag{B4}$$

Dividing both sides of (B4) by the left-hand one gives

$$1 = \frac{k_1}{n} \frac{(Z_1+Z_2-n+1)}{(Z_1-k_1+1)} \frac{(Z_1-k_1+1)}{(Z_1+Z_2-n+1)} + \frac{(n-k_1)}{n} \frac{(Z_1+Z_2-n+1)}{(Z_2-n+k_1+1)} \frac{(Z_2-n+k_1+1)}{(Z_1+Z_2-n+1)} = \frac{k_1}{n} + \frac{n-k_1}{n} = 1 . \tag{B5}$$

The identity we have proves that (B3) is indeed a solution and it is straightforward to check that the factor $\binom{Z_1+Z_2}{Z_1}$ in the denominator of (B3) provides for the proper normalization.

The moments of the distribution $P_{k_1}^n$ can be calculated using the identity

$$\sum_{k_1} \begin{bmatrix} n \\ k_1 \end{bmatrix} \begin{bmatrix} m-n \\ l_1-k_1 \end{bmatrix} = \begin{bmatrix} m \\ l_1 \end{bmatrix} , \tag{B6}$$

which can be easily proved by developing both sides of the identity

$$(a+b)^n (a+b)^{m-n} = (a+b)^m .$$

The first moment is given by

$$\langle k_1 \rangle = \frac{1}{\begin{bmatrix} Z_1+Z_2 \\ Z_1 \end{bmatrix}} \sum_{k_1} k_1 \begin{bmatrix} n \\ k_1 \end{bmatrix} \begin{bmatrix} Z_1+Z_2-n \\ Z_1-k_1 \end{bmatrix} = \frac{n}{\begin{bmatrix} Z_1+Z_2 \\ Z_1 \end{bmatrix}} \sum_{k_1'} \begin{bmatrix} n-1 \\ k_1' \end{bmatrix} \begin{bmatrix} Z_1+Z_2-n \\ Z_1-k_1'-1 \end{bmatrix} , \tag{B7}$$

where $k_1' = k_1 - 1$. Using (B6) we get

$$\langle k_1 \rangle = \frac{n}{\begin{bmatrix} Z_1+Z_2 \\ Z_1 \end{bmatrix}} \begin{bmatrix} Z_1+Z_2-1 \\ Z_1-1 \end{bmatrix} = \frac{nZ_1}{Z_1+Z_2} . \tag{B8}$$

Calculation of the second moment is accomplished by first rewriting it as the following:

$$(M_2)_1 = \langle k_1^2 \rangle - (\langle k_1 \rangle)^2 = \langle k_1(k_1-1)+k_1 \rangle - (\langle k_1 \rangle)^2 = \langle k_1(k_1-1) \rangle - \langle k_1 \rangle (\langle k_1 \rangle - 1) . \tag{B9}$$

Calculation of $\langle k_1(k_1-1) \rangle$ is done in the same fashion as the calculation of $\langle k_1 \rangle$ in (B7) and (B8) and the final result for $(M_2)_1$ is

$$(M_2)_1 = \frac{nZ_1Z_2(Z_1+Z_2-n)}{(Z_1+Z_2)^2(Z_1+Z_2-1)} . \tag{B10}$$

The result from (B8) can be used to write $(M_2)_1$ in the more convenient form

$$(M_2)_1 = \frac{\langle k_1 \rangle \left[1-\frac{\langle k_1 \rangle}{n}\right] \left[1-\frac{\langle k_1 \rangle}{Z_1}\right]}{\left[1-\frac{\langle k_1 \rangle}{nZ_1}\right]} . \tag{B11}$$

The case that is treated in the paper is more complicated than the one discussed until now as it includes a probability for the electron not to get caught into any of the ions. Such a case may be described by the new set of probabilities,

$$\Pi_1 = \frac{(1-\epsilon)(Z_1-k_1)}{Z_1+Z_2-(1-\epsilon)(k_1+k_2)} ,$$
$$\Pi_2 = \frac{(1-\epsilon)(Z_2-k_2)}{Z_1+Z_2-(1-\epsilon)(k_1+k_2)} , \tag{B12}$$
$$\Pi_3 = 1-\Pi_1-\Pi_2 ,$$

where ϵ determines the escape probability and Π_1 and Π_2 have the same meaning as before. Π_3 is the escape probability for an electron after Z_1 and Z_2 caught k_1 and k_2 electrons, respectively. Assuming that we focus our attention on Z_1, and are not interested in the number of electrons caught into Z_2, we can describe the process by only two probabilities

$$\tilde{\Pi}_1 = \Pi_1 = \frac{(1-\epsilon)(Z_1-k_1)}{Z_1+Z_2-(1-\epsilon)(k_1+k_2)} ,$$
$$\tilde{\Pi}_2 = 1-\tilde{\Pi}_1 = \frac{\epsilon(Z_1+Z_2)+(1-\epsilon)(Z_2-k_2)}{Z_1+Z_2-(1-\epsilon)(k_1+k_2)} . \tag{B13}$$

Now we can define a new "pseudocharge" for ion Z_2 by

$$\tilde{Z}_2 = \frac{Z_2+\epsilon Z_1}{1-\epsilon} . \tag{B14}$$

Substitution of (B14) into (B13) brings the probabilities into the form

$$\tilde{\Pi}_1 = \frac{Z_1-k_1}{Z_1+\tilde{Z}_2-(k_1+k_2)} ,$$
$$\tilde{\Pi}_2 = \frac{\tilde{Z}_2-k_2}{Z_1+\tilde{Z}_2-(k_1+k_2)} , \tag{B15}$$

which is the same form as (B1) with $\tilde{Z}_2$ substituted for Z_2. Therefore all the results derived from (B1) are true for (B15), with the same substitution. Specifically the first moment of $\langle k_1 \rangle$ is given by

$$\langle k_1 \rangle = \frac{nZ_1}{Z_1+\tilde{Z}_2} = \frac{nZ_1(1-\epsilon)}{Z_1+Z_2} \tag{B16}$$

and the form (B11) for $(M_2)_1$ which does not depend explicitly on Z_2, does not change at all.

---

*Present address: Department of Physics, Brookhaven National Laboratory, Upton, NY 11973.

[1]H. D. Betz, Rev. Mod. Phys. 44, 465 (1972).
[2]H. D. Betz, in *Atomic Physics in Nuclear Experiments,* edited by B. Rosner and R. Kalish (Hilger, London, 1977), p. 255.
[3]J. H. McGuire and L. Weaver, Phys. Rev. A 16, 41 (1977).
[4]V. V. Afrosimov and N. V. Fedorenko, Sov. Phys.—Tech. Phys. 2, 2378 (1957).
[5]E. Everhart and Q. C. Kessel, Phys. Rev. Lett. 14, 247 (1965).
[6]U. Fano and W. Lichten, Phys. Rev. Lett. 14, 627 (1965).
[7]J. D. Garcia, R. J. Fortner, and T. M. Ravanagh, Rev. Mod. Phys. 45, 111 (1973).
[8]Q. C. Kessel and B. Fastrup, Case Stud. At. Phys. 3, 137 (1973).
[9]J. S. Briggs, Rep. Prog. Phys. 39, 217 (1976).
[10]M. Meron, D. Maor, and B. Rosner, Phys. Lett. 74A, 201 (1979).
[11]M. Meron, D. Maor, and B. Rosner, J. Phys. B 16, 3983 (1983).
[12]B. Rosner and D. Gur, Phys. Rev. A 15, 70 (1977).
[13]D. Maor and B. Rosner, Phys. Lett. 69A, 100 (1978).
[14]B. Rosner and W. Brandt, Phys. Lett. 61A, 97 (1977).
[15]V. F. Weisskopf and D. H. Ewing, Phys. Rev 57, 472 (1940).
[16]B. Rosner, D. W. Mingay and E. Barnard, S. Afr. J. Phys. 6, 1 (1983).
[17]A. Russek and M. Thomas, Phys. Rev. 109, 2015 (1958).
[18]A. Russek and J. Meli, Physica (Utrecht) 46, 222 (1970).
[19]G. N. Watson, *A Treatise on the Theory of Bessel Functions,* 2nd ed. (Cambridge University Press, Cambridge, 1958).